Capacity of Anchors in Structural Connections

T. Cornelius and G. Secilmis

Abstract—When dealing with safety in structures, the connections between structural components play an important role. Robustness of a structure as a whole depends both on the load-bearing capacity of the structural component and on the structures capacity to resist total failure, even though a local failure occurs in a component or a connection between components. To avoid progressive collapse it is necessary to be able to carry out a design for connections. A connection may be executed with anchors to withstand local failure of the connection in structures built with prefabricated components. For the design of these anchors, a model is developed for connections in structures performed in prefabricated autoclaved aerated concrete components. The design model takes into account the effect of anchors placed close to the edge, which may result in splitting failure. Further the model is developed to consider the effect of reinforcement diameter and anchor depth. The model is analytical and theoretically derived assuming a static equilibrium stress distribution along the anchor. The theory is compared to laboratory test, including the relevant parameters and the model is refined and theoretically argued analyzing the observed test results. The method presented can be used to improve safety in structures or even optimize the design of the connections.

Keywords—Robustness, anchors, connections, aircrete, prefabricated components.

I. INTRODUCTION

THE demand for calculation methods for aircrete structures is increasing due to the growing use of autoclaved aerated concrete in constructions, in the following denoted aircrete. It was decided to develop a model for designing the load-bearing capacity of anchors in connections between prefabricated aircrete components, to resist progressive collaps. Often progressive collaps may be avoided having sufficient loadbearing capacity in the connections, see for instance [1]-[3].
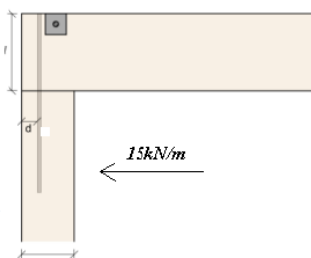

Fig. 1 Anchor connection between floor element and wall element

T. Cornelius, is with the Danish Building Research Institute, Aalborg University, 2450 Copenhagen, Denmark (phone: (+45)99402280; email: tcb@sbi.aau.dk).

Güney Secilmis, is with the Danish Building Research Institute, Aalborg University, 2450 Copenhagen, Denmark (phone: (+45)99402356; email: gse@sbi.aau.dk).

A joint between an aircrete wall and aircrete floor components in a typical multiple story building is analyzed, taking into account the accident load, see Fig. 1. The setting depth of an anchor is assumed to be equal to the thickness of the floor component to ensure maximum utilization of the aircrete area. The load from storey above is ignored because that they act in favor. The vertical anchor is considered as a thread rod glued into the floor element.

II. TEST RESULTS

A series of 31 tests was carried out to examine the behavior of anchors in aircrete. Two failure modes we observed: local spalling of the top of the test specimen, see Fig. 2 and crushing of the aircrete in front of the reinforcing anchor finally resulting in total spalling through the specimen, see Fig. 3. Similarly failure modes may be found in [4]-[6].
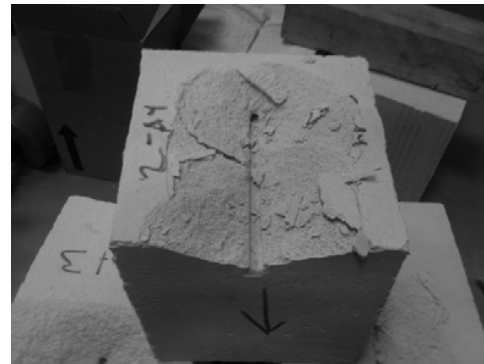

Fig. 2 Local Spalling

Fig. 3 Total spalling, crushing in front of reinforcement

The test setup is shown in Figs. 4 and 5. The specimen is shown on the left side of Figs. 4 and 5. The specimen is secured using screws on all 4 sides stabilizing the specimen to ensure maximum test accuracy. At point C, a hydraulic jack is

placed and in between the hydraulic jack and the anchor a measurement instrument is placed to get a reading. At point C, in Fig. 4, the anchor was placed under a circular component, which is fastened to a wooden base using a bolt and a nut. This circular element ensures zero torque in point C Fig. 4. The steel plates placed over and under the bolt as seen in Fig. 5 are placed in order to ensure a balanced distribution of forces.

The specimens all have the dimensions 20cmx20cmx20cm, but two different aircrete test series were performed with compressive strengths of 2.0MPa and 4.0MPa respectively and related uniaxial tensile strength of 0.24MPa to 0.55MPa. The specimens labeled with an *a* in Table I represents high strength values and specimens labeled with a *b* in Table I represents low strength values.

Fig. 4 Test Setup

The following parameters are varied in test specimens: ϕ which is the diameter of the anchor, l_3 is the setting depth indicating how deep the anchor is inserted into the specimen and d is the edge distance measured from the anchor to the edge of the specimen. Furthermore, the distances l_1, l_2, l_3 and l_4 describe the distances between the test setup elements, which are, l_1 the distance between the hydraulic jack and the wooden base l_2 which is the distance between the specimen and the hydraulic jack, l_3 represents the setting depth and l_4 which is the distance between the specimen and P_E.
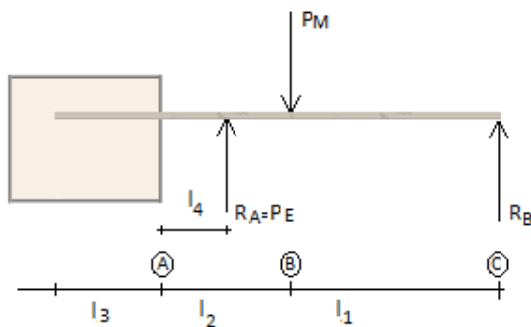

Fig. 5 Test Setup

The test specimen is loaded by the force, P_M, which is measured. This leads to reactions R_A and R_B where $R_A = P_E$ is the equivalent force of the constraint forces in the test specimen.

Test results applied in this analysis are presented in Table I. The measured value is denoted P_M, see Fig. 4. P_E is the equivalent force replacing the reactions in the specimen inflicted to cause failure, P is the decisive force in the specimen, see Fig. 6.

TABLE I
TEST RESULTS

	P_M kN	P_E kN	P kN	ϕ mm	l mm	d mm
1-a	0.92	1.02	2,04	8	150	30
2-a	2.43	2.91	5,82	8	190	50
3-a	2.10	2.51	5,03	8	190	50
4-a	0.95	1.16	2,32	6	200	30
5-a	1.58	1.93	3,86	8	200	30
6-a	0.70	0.85	1,71	8	200	10
7-a	1.56	1.90	3,81	8	200	30
8-a	2.10	2.56	5,13	8	200	30
9-a	1.45	1.26	2,51	8	100	30
10-a	2.10	1.82	3,64	8	100	30
11-a	1.80	1.56	3,12	8	100	30
12-a	2.77	2.88	5,76	8	200	90
13-a	3.20	3.02	6,05	10	150	90
14-a	2.67	2.52	5,05	10	150	70
15-a	1.24	1.17	2,34	10	150	30
16-a	2.59	2.45	4,90	10	150	50
17-a	1.49	1.41	2,82	12	150	70
18-a	1.59	1.65	3,31	8	200	70
19-a	2.06	1.78	3,57	8	100	70
20-a	1.27	1.10	2,20	8	100	50
21-a	0.94	0.81	1,63	8	100	30
22-a	1.79	1.69	3,38	8	150	70
1-b	1.49	1.41	2,82	10	150	70
2-b	0.39	0.37	0,74	10	150	30
3-b	0.83	0.78	1,57	10	150	50
4-b	0.77	0.73	1,46	8	150	70
5-b	1.74	1.64	3,29	12	150	70
6-b	0.89	0.93	1,85	8	200	70
8-b	0.63	0.55	1,09	8	100	50
9-b	0.38	0.33	0,66	8	100	30
10-b	1.04	0.98	1,97	8	150	70

III. THEORY

Several investigations have been done. For an overview see [7] which describes several typical failure modes for anchors in concrete.

In order to develop the model for calculating the capacity of anchors in structural connections, we assume a stress distribution must be set. The model is based on the assumption that the anchor can resist the load as a torque affected pole anchored in the aerated concrete. It is expected that a tension distribution between a plastic distribution and an elastic distribution will occur. In relation to this, a plastic distribution model and an elastic distribution model are established for the stress distribution.

Assuming an elastic distribution, the load-bearing area is determined by vertical equilibrium, given that the force applied to the anchor and strength of the aircrete is known.
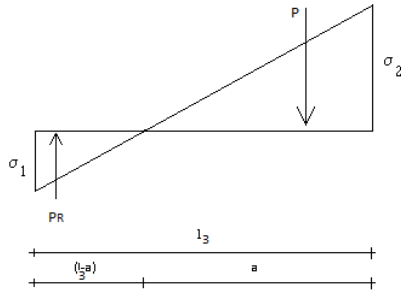
Fig. 6 Elastic stress distribution on the anchor loaded by the external force P

$$P = 0.5 \cdot \sigma_2 \cdot \phi \cdot a \tag{1}$$

Solving equilibrium equations for the elastic solutions we find:

$$a = \frac{2}{3} l_3 \tag{2}$$

fulfills the capacity criteria:

$$\sigma_2 \leq k \cdot f_c \tag{3}$$

where k is the concentrated load factor accordingly to [8] and [9], see Table II:

TABLE II
CONCENTRATED LOAD FACTOR

	Aircrete	Concrete
k	3,3	3,0

and hereby we get the loadbearing capacity in (4):

$$P = \frac{1}{3} \cdot \phi \cdot l_3 \cdot k \cdot f_c \tag{4}$$

Similarly using a plastic distribution we get:

$$a = \frac{l_3}{\sqrt{2}} \tag{5}$$

and hereby:

$$P = \frac{l_3}{\sqrt{2}} \cdot \phi \cdot l_3 \cdot k \cdot f_c \tag{6}$$

Observing Fig. 6 we may replace P and P_R with an equivalent force P_E which from vertical projection gives:

$$P_E = P - P_R \tag{7}$$

and assuming elastic distribution we have $P = 2P_R$ leading to:

$$P = 2P_E \tag{8}$$

Further the stress distribution in the test specimen gives a torque, which results in the equivalent force P_E located outside the specimen in a distance l_4, see Fig. 5, of:

$$l_4 = \frac{4}{9} l_3 \tag{9}$$

We hereby get the relation between the measured force P_M and the equivalent force P_E:

$$P_E = P_M \frac{l_1}{((l_2 - l_4) + l_1)} \tag{10}$$

and hence using (4) and (8) we may determine the load bearing capacity P.

The plastic distribution is expected to be on the unsafe side giving high loadbearing capacities. The model for crushing failure will be replaced by the split theory asserting itself for low distances between the anchor and the edge. The split theory takes into consideration the low utilization of the aircrete area and the alternative fracture pattern occurs when the edge distance is low.

The capacity of anchors in structural connections, with low edge distances may result in spalling failure as shown in Fig. 2. Assuming that spalling failure may be estimated by a splitting failure determined by using (11), see [10]:

$$\bar{p} = \frac{1}{2} \pi f_t d \tag{11}$$

where p is the equivalent line load correlated by the actual stress distribution, see for example elastic distribution in Fig. 6 spread over the length a = 2/3l by (12):

$$\bar{p} = \alpha \cdot \frac{P}{a} = \alpha \frac{3}{2} \frac{P}{l_3} \tag{12}$$

where the factor $\alpha = 1.0$ corresponding to pure plastic distributed stress rising to $\alpha = 2.0$ in the case of elastic stress distribution.

Combining (11) and (12) we then get the derived splitting capacity given in (13):

$$P = \frac{1}{3\alpha} \pi \cdot f_t \cdot dl_3 \tag{13}$$

observing that for increasing α value we obtain lower loadbearing capacity.

IV. ANALYSIS

The test data were compared to the developed theory using regressions analysis and determining the variance on the data. Initially it was observed that the test data fitted approximately assuming an elastic stress distribution. Comparing all tests to

the theory for crushing failure it was observed that as expected there was a clear difference between data with low and high edge distance d, see Fig. 7.
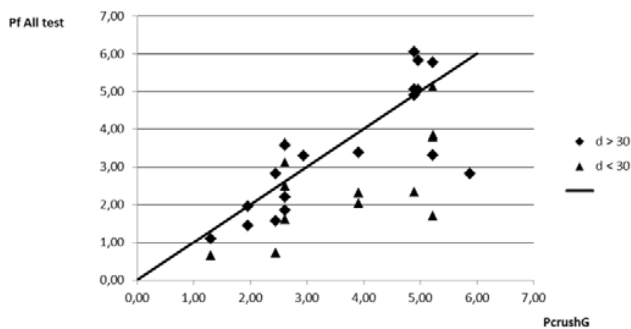

Fig. 7 Test results versus theory for crushing of the aircrete

In the further analysis the test data where analyzed separately depending on an edge distance larger or smaller than 30mm. In the analysis of test data with edge distance larger than 30mm, an optimum comparing with crushing failure, see (4) was found introducing a factor of $\beta = 0.75$ reducing the coefficient of variance from 0.27 to 0.15. Some of this reduction may be explained by the stress distribution not being perfectly elastic, but the main explanation is probably found in the fact that the test were performed with rods, which do have a lower stiffness and a relatively lower effective diameter, due to the threads. To clarify this three test samples was carried out with cast smooth steel bars, and these tests clearly showed a higher load-bearing capacity, see upper data in Fig. 8.
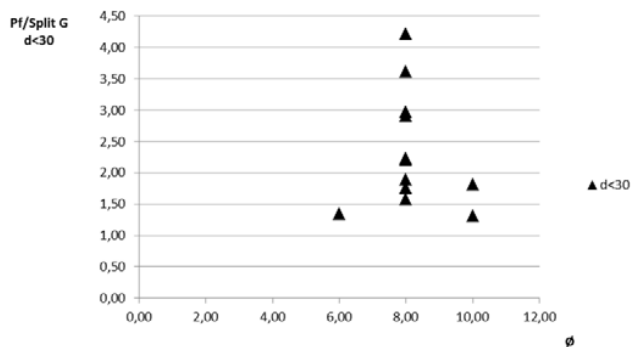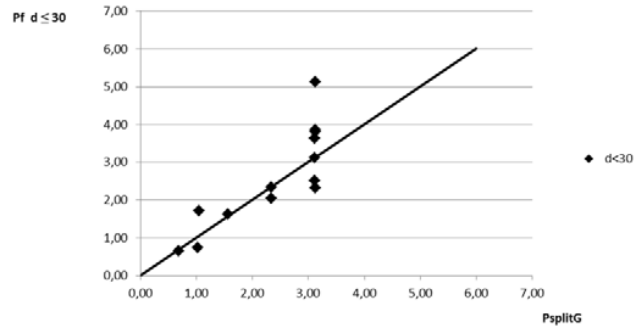

Fig. 8 Test results for edge distance d < 30mm

Fig. 9 Test results versus theory for edge distance d < 30 mm

Analyzing the test data and comparing them to the splitting theory optimizing the stress distribution α from (13) on both the smooth steel bars and the threaded rods, the stress distribution factor α was optimized achieving a change in variance from 0.59 to 0.15 using $\alpha = 1.1$ on threaded rods indicating the stress distribution approaches a plastic stress distribution before failure in the case of splitting, see results in Fig. 9.

V. CONCLUSION

It has been shown that the theories developed for the two types of failure mode, crushing and spalling correlates satisfactorily with the test performed obtaining a variance of about than 0.15 in both failures, which may be considered sufficiently statistically verified for these types of test.

It is further assumed and verified that it is possible to approximate with an elastic/plastic stress distribution.

Finally it was observed that there was a significant difference between using smooth steel bars and threaded rods, and even though the difference is minor further investigation is recommended in the future.

REFERENCES

[1] S. Kokot, "Progressive collaps - structure of industrial plastics". Ispra,Italy Elsevier 2012.
[2] B.A. Izzudin, "Progressive collapse of mulit-storey buildings due to sudden column loss". London, United Kingdom Elsevier 2007.
[3] A.G. Vlassis, "Progressive collapse of multistory building due to failed floor impact". London, United Kingdom Elsevier 2009.
[4] Ivan Gomez, Amit Kanvinde, Chris Smith and Gregory Deierlein, "Shear transfer in exposed base plates," *American Institute of Steel Construction*, 2009
[5] Ö. Çalışkan, S. Yılmaz, H. Kaplan and N. Kıraç, "Shear strength of epoxy anchors embedded into low strength," *Construction and Building Materials 38, Elsevier*, Sep. 2012 concrete
[6] Y. Zhang, "Dynamic behavior of multiple-anchor connections in cracked concrete," *Ph.D Dissertation, University of Texas at Austin*, Apr. 1997
[7] R. Eligehausen, Rainer Mallée and John F. Silva, "Anchorage In Concrete Construction", *Ernst & Sohn*, 2006

[8] TC250, "EN1992-1-1, Eurcode 2 - Design of concrete structures – part 1-1, general rules and rules for building", *CEN*, Brussels, Belgium 2004.
[9] TC177, "EN12602 - Prefabricated reinforced components of autoclaved aerated concrete", *CEN*, Brussels, Belgium 2008.
[10] F. L. L. B. Carneiro, and A.BAHCELLOS, "Tensile Strength of Concretes." R.I.L.E.M. Bulletin No. 13, Mar. 1953, pp. 9%125.